Journal of The Electrochemical Society, **153** (2) G128-G133 (2006)
0013-4651/2005/153(2)/G128/6/$20.00 © The Electrochemical Society

Oxide Grown on Polycrystal Silicon by Rapid Thermal Oxidation in N_2O

Chyuan Haur Kao,[a] Chao Sung Lai,[a,z] and Chung Len Lee[b]

[a]*Department of Electronics Engineering, Chang Gung University, Kwei-Shan, Tao Yuan, Taiwan*
[b]*Department of Electronics Engineering, National Chiao Tung University, Hsinchu, Taiwan*

In this paper, rapid thermal processing (RTP) N_2O polyoxides were studied in terms of oxidation temperature and thickness with O_2 oxidation polyoxides as comparison. Atomic force microscopy, transmission electron microscopy, and secondary ion mass spectroscopy measurements were employed to correlate the electrical characteristics with the physical structures. Results showed that RTP N_2O-grown polyoxides exhibited better characteristics on the leakage current, E_{bd}, trappings and Q_{bd}. It was found that it was the proper amount of nitrogen incorporated in the polyoxide improving the interface of the polyoxide/polysilicon, consequently improving the electrical quality. The initial hole-trapping phenomenon during the constant current stress, which was due to the incorporated nitrogen, was also observed in the N_2O-grown polyoxides. The two-step RTP process, i.e., first RTP oxidizing the polysilicon in O_2 and then RTP oxidizing in N_2O, could achieve polyoxide of good characteristics by incorporating the proper amount of nitrogen into the polyoxide.
© 2005 The Electrochemical Society. [DOI: 10.1149/1.2138671] All rights reserved.

Manuscript submitted May 26, 2005; revised manuscript received September 15, 2005.
Available electronically December 23, 2005.

Thermal oxides grown on n^+-doped polysilicon (polyoxides) have been widely used in nonvolatile memories such as EPROM, EEPROM, and flash EEPROM cells.[1-4] Of particular importance in most applications is that the polyoxides exhibit a low leakage current and a high breakdown field. The breakdown strength is strongly influenced by the smoothness of the polyoxide/polysilicon interface.[5,6] According to previous studies,[7-9] the electrical properties of the polyoxides have been shown to depend on the polysilicon deposition temperature, doping process, and oxidation temperature. Also, the difference in the degree of roughness at the top and bottom interfaces causes the bias-polarity dependence of the current-field characteristics. In order to obtain good data retention characteristics, the polyoxide with low conductivity and high breakdown fields have long been sought.[10-13] More importantly, some floating-gate nonvolatile memories that rely on electron tunneling through the polyoxides require a high charge to breakdown (Q_{bd}) and low trapping rate during programming and erasing operations.[14]

It was reported that more reliable dielectrics could be grown on polysilicon by using deposited instead of thermally grown polyoxides. For those chemical vapor deposited (CVD) dielectrics, the grain boundaries present in the bottom polysilicon are not incorporated in the deposited layer due to no polysilicon consumption. The surface of the polysilicon layer is not roughened, so the CVD oxide potentially has a defect density relatively independent of the bottom polysilicon.[15-18]

N_2O used as an oxidant or a postoxidation annealing ambient for the gate dielectrics grown on single-crystal Si has received much attention due to its endurance to Fowler-Nordheim (F-N) stress. This is attributed to the incorporation of nitrogen at the oxide/silicon–substrate interface.[19,20] It has been shown that N_2O-grown oxide exhibits reduced electron trappings, superior breakdown properties, and suppressed interface state generation under the hot-carrier stress, as compared to pure SiO_2.[21] Recently, N_2O was applied to grow polyoxide on n^+-polysilicon in the oxidation furnace[22] to obtain polyoxide of better integrity, also due to incorporation of nitrogen in polysilicon grain boundaries to form oxynitride. The oxynitride formed reduces the enhanced oxidation effect of grain boundaries to make the polyoxide/poly-1 interface smoother.

In this paper, we applied the N_2O oxidation to n^+doped polysilicon to grow polyoxides by using rapid thermal processing (RTP) and studied the electrical characteristics of the grown polyoxides. The study was in terms of the oxidation temperature and thickness with O_2 oxidation samples as comparison. Atomic force microscopy (AFM), transmission electron spectroscopy (TEM), and secondary ion mass spectroscopy (SIMS) measurements were employed to correlate electrical characteristics with the physical structures. Results showed that N_2O samples exhibited better characteristics than O_2-grown samples; however, as the oxidation temperature was increased, the electrical characteristics of N_2O samples became degraded, even though they still showed superior characteristics than the O_2-grown samples. Also, the hole-trapping phenomenon was observed in the N_2O-grown polyoxides. In addition, the two-step RTP oxidation, i.e., first RTP oxidizing the polysilicon in O_2 then in N_2O, was studied. Improved characteristics were obtained. With all the experimental data, it is concluded that to obtain improved characteristics by using the N_2O rapid thermal oxidation, only an appropriate amount of nitrogen should be incorporated.

Experimental

In this study, n^+-polysilicon/polyoxide/n^+-polysilicon capacitors were fabricated. At first, p-type wafers were thermally oxidized to have a field oxide of a thickness of 100 nm. All samples were then deposited on a 300-nm polysilicon film at 620°C and doped with $POCl_3$ at 875°C. The sheet resistance of the film was 85 $\Omega/\square$. Then, interpolyoxides with a thickness of the range 85–200 Å were grown on the polysilicon films at 950–1050°C for time ranging from 50 to 500 s in a pure N_2O ambient by using an AG610 RTP processor. For comparison, polyoxides with a thickness of 115 Å were grown at 950 and 1050°C for 180 and 50 s, respectively, in a pure O_2 ambient, also by RTP. The flow rate for N_2O and O_2 was all 3 slm. In order to study the N_2O annealing effect, samples were first oxidized with RTP at 950°C for 180 s in the pure O_2 ambient and then annealed in the N_2O ambient at 950°C for 90 s with RTP. The final thickness of the oxide was about 155 Å. After the interpolyoxide formation, a second polysilicon film (poly-2) of about 300 nm was deposited which was doped by $POCl_3$ to a sheet resistance of 85 $\Omega/\square$. After poly2 was patterned, all samples were grown on a 100-nm-thick oxide via wet oxidation at 850°C. Contact holes were opened and metallized to form the capacitor structure. Finally, all devices were sintered at 350°C for 40 min in the N_2 gas, which can improve the metallurgy between polysilicon and metal film with reduced resistance.

Polyoxide thickness was determined by the high-frequency (1 MHz) using Keithley capacitance-voltage (C-V) measurements. The morphology of the polyoxide/polysilicon interface was studied by TEM and AFM. For the AFM measurement of the surface, to reveal the polyoxide/poly-1 interface, the polyoxide layer was removed by wet etching in the buffered HF acid. The true replica of the interface may be preserved by such a treatment because the

[z] E-mail: cslai@mail.cgu.edu.tw

Downloaded on 2014-04-26 to IP 140.113.38.11 address. Redistribution subject to ECS terms of use (see ecsdl.org/site/terms_use) unless CC License in place (see abstract).

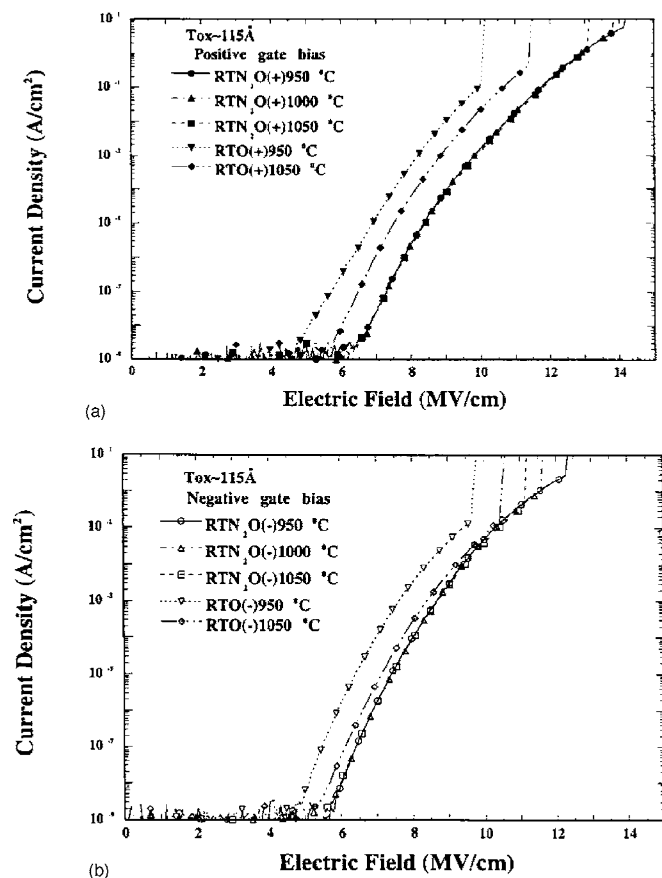

Figure 1. J-E characteristics of the N_2O-grown and O_2-grown polyoxides of a thickness of 115 Å grown at 950, 1000, and 1050°C for the top gate applied at (a) a positive and (b) negative bias, respectively.

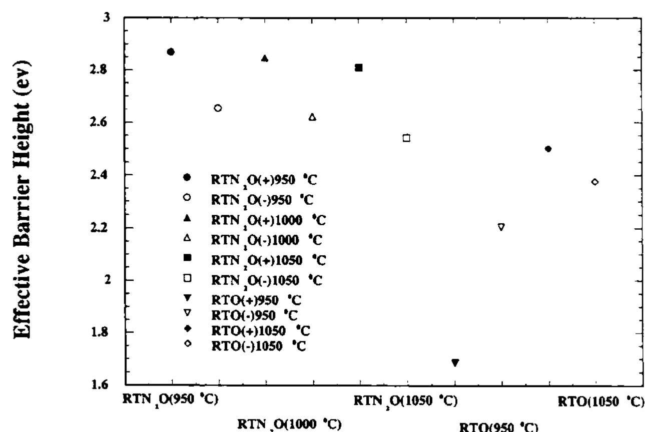

Figure 2. Effective barrier height, ϕ_b, of the N_2O-grown and O_2-grown polyoxides grown at temperatures of 950–1050°C.

poly-Si is not attacked by the HF-based solution.[23] The current-voltage (I-V) characteristics were measured by using an HP4145B semiconductor parameter analyzer.

Results and Discussion

Figure 1a and b shows the typical positive and negative J-E characteristics of the N_2O-grown and O_2-grown polyoxides with the thickness of 115 Å grown at the temperature of 950, 1000, and 1050°C, respectively. It can be seen that the N_2O-grown polyoxides conducted a lower leakage current and a higher breakdown electric field than those of the O_2-grown polyoxides for both the positive and negative gate biases. For the O_2-grown polyoxides, the J-E characteristics were improved for the higher growth temperature. However, for the N_2O-grown polyoxides, the dielectric breakdown field (E_{bd}) degraded as the growth temperatures increased. For both polyoxides, the positive characteristics were better than the negative characteristics. Shown in Fig. 2 is the derived values of the effective barrier height, ϕ_b, of the O_2-grown polyoxide and N_2O-grown polyoxide where the effective electron mass within the polyoxide bandgap has been taken as 0.5 m_0 (m_0: free electron mass). As expected, the barrier heights of the N_2O-grown polyoxides were all higher than those of the O_2-grown polyoxides. This indicates that the N_2O-grown polyoxides had smoother poly-1/polyoxide surfaces than those of the O_2-grown polyoxides. Furthermore, for the N_2O-grown polyoxide, the barrier heights of the positive characteristics (injection from the polyoxide/poly-1 interface) were better than those of the negative characteristics (injection from the poly-2/polyoxide interface). This seems to indicate that the bottom poly-1/polyoxide interface is smoother than the top poly-2/polyoxide interface for the N_2O-grown polyoxide. However, for the O_2-grown polyoxides, their barrier heights were improved for the higher oxidation temperature, which may be due to smoother interface at the higher oxidation temperature of 1050°C. For the N_2O-grown polyoxides, their barrier heights slightly degraded for the higher growth temperature. The above J-E characteristics may be related with the morphology of the polyoxide/polysilicon interfaces.

In order to investigate the actual morphology of the interface between the polyoxide and polysilicon, AFM measurements were performed for the polyoxides. Figure 3a and b shows the AFM images of the surfaces of the N_2O-grown polyoxides grown at temperatures of 950 and 1050°C, and the average roughness (*Ra*) values of AFM are 35.8, and 37.2 Å, respectively. Figure 3c and d shows the same pictures for the O_2-grown polyoxides grown at the same temperatures of 950 and 1050°C, and the average roughness (*Ra*) values of AFM are 51 and 39.6 Å, respectively. It can be seen that the N_2O-grown polyoxides with lower *Ra* values had smoother poly-1/polyoxide surfaces than those of the O_2-grown polyoxides. This smoother surface of the N_2O-grown polyoxide can be attributed to the nitrogen diffusing into grain boundaries and reducing the grain boundary enhancement effect. Furthermore, for the N_2O-grown samples, the 950°C sample had a slightly smoother interface than that of the 1050°C sample, which may be due to excessive nitrogen during higher oxidation temperature incorporated into polyoxide/polysilicon interface to induce larger thickness nonuniformity[24] across the wafer, despite a locally smoother surface. For the O_2-grown samples, the 1050°C sample had a smoother interface than that of the 950°C sample due to operating of viscous flow of SiO_2 and polysilicon, and diffusion controlled at higher oxidation temperature. Cross-sectional TEM micrographs were also taken for the above samples. They are shown in Fig. 4a and b for the 950 and 1050°C N_2O-grown samples, respectively, and in 4c and d for the 950 and 1050°C O_2-grown samples, respectively. We can see that the N_2O-grown polyoxides had larger grain sizes on the poly-1 and smoother polyoxide/poly-1 interfaces than those of the O_2-grown polyoxides. Furthermore, for the N_2O-grown polyoxides, the bottom poly-1 film had more uniform distribution and larger grain sizes than those of the top poly-2 film. This seems to indicate the bottom poly-1/polyoxide interface is smoother than the top poly-2/polyoxide interface as barrier height revealed. However, for the N_2O-grown polyoxides, the 950°C sample had a slightly smoother polyoxide/polysilicon interface than that of the 1050°C sample (see Fig. 4a and b). For the O_2-grown polyoxides, the 1050°C sample had a smoother polyoxide/polysilicon interface than that of the 950°C sample (see Fig. 4c and d).

The slightly smoother surfaces of the N_2O-grown polyoxides can be attributed to the nitrogen, which diffused along and into grain boundaries of the polysilicon to form oxynitride at grain boundaries,

Downloaded on 2014-04-26 to IP 140.113.38.11 address. Redistribution subject to ECS terms of use (see ecsdl.org/site/terms_use) unless CC License in place (see abstract).

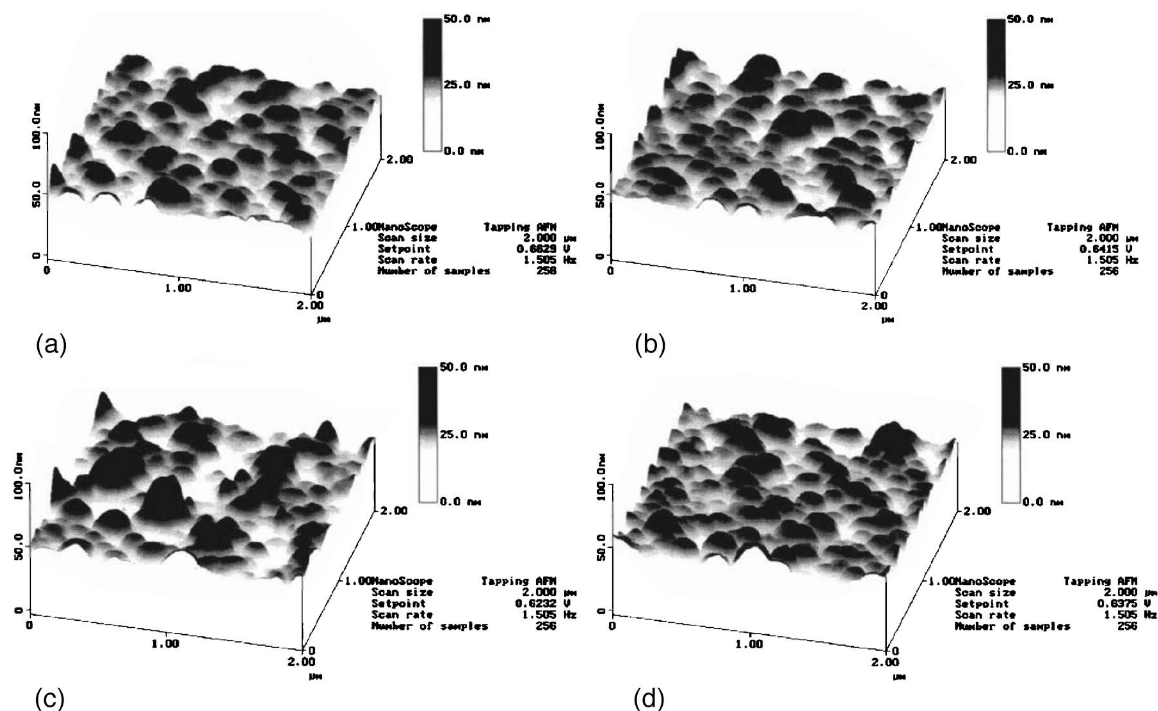

Figure 3. AFM images of the poly1 surfaces of (a) the N_2O-grown polyoxide at 950°C, (b) the N_2O-grown polyoxide at 1050°C, (c) the O_2-grown polyoxide at 950°C, and (d) the O_2-grown polyoxide at 1050°C.

and the oxynitride reduced the enhanced oxidation effect of grain boundaries.[25] However, too much nitrogen induces larger thickness nonuniformity across the wafer, despite a locally smoother surface. Figure 5 shows the thickness distributions of polyoxides parallel to the wafer flat surface from the center to the two edges for the O_2-grown and N_2O-grown polyoxides, which had nearly the same thickness at the center. It can be seen that the thickness deviation was only 3–4 Å (3%) for the O_2-grown polyoxide but was about 15 Å (13%) for the N_2O polyoxide grown at 950°C, increasing to 32 Å (27%) for the N_2O polyoxide grown at 1050°C.

The charge trapping characteristics of the polyoxides were investigated. Figure 6 shows the curves of gate voltage shift (ΔV_g) vs time for both the N_2O-grown and the O_2-grown polyoxides under a constant ±10 mA/cm^2 current stress. The area of the test capacitor was 5×10^{-4} cm^2. In the figure, the 950°C O_2-grown polyoxide exhibited the largest electron trapping rates in both polarity stresses. As the temperature increased, the trapping rates decreased. For the N_2O-grown polyoxides, it can be seen that initial hole trappings occurred under the positive constant current stress for all the samples and the higher the growth temperature, the larger the hole trapping rate.[26] For the negative stress, electron trapping rates were lower than those of the O_2-grown polyoxides. These results were similar to those found for the oxides grown in N_2O and O_2 mixtures

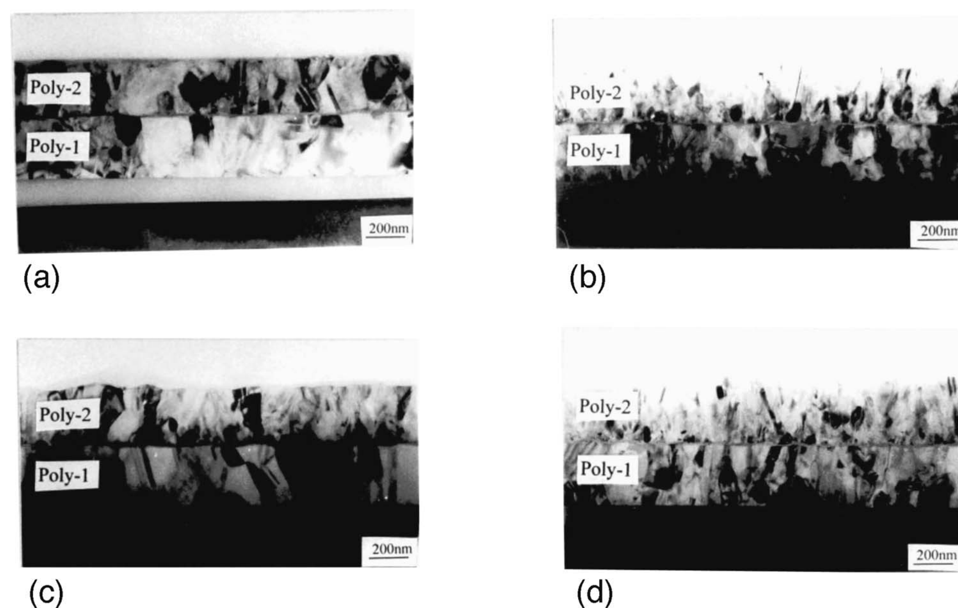

Figure 4. Cross-sectional TEM micrographs of (a) N_2O-grown polyoxide at 950°C, (b) N_2O-grown polyoxide at 1050°C, (c) O_2-grown polyoxide at 950°C, and (d) O_2-grown polyoxide at 1050°C.

Downloaded on 2014-04-26 to IP 140.113.38.11 address. Redistribution subject to ECS terms of use (see ecsdl.org/site/terms_use) unless CC License in place (see abstract).

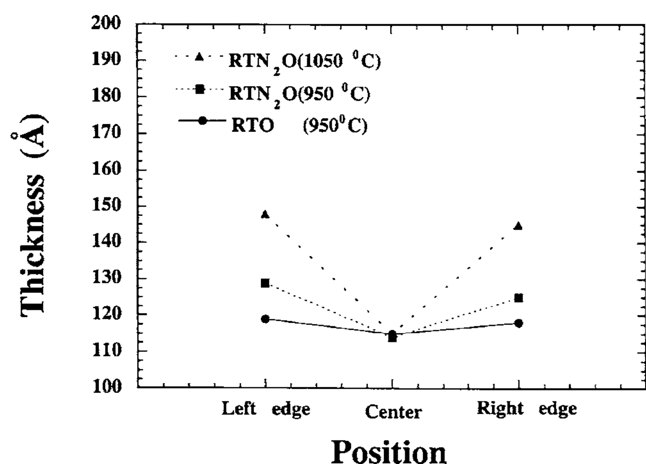

Figure 5. Measured distribution of the polyoxide thickness parallel to the wafer flat surface from the center to the two edges with nearly the same thickness at the center for the N_2O-grown and O_2-grown polyoxides.

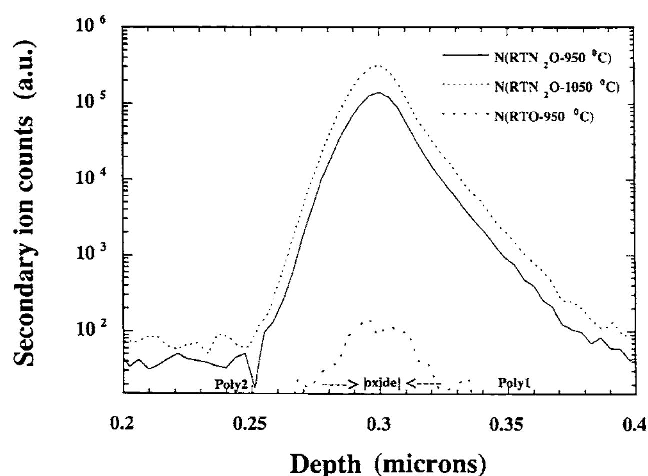

Figure 7. SIMS nitrogen profiles of the N_2O-grown and O_2-grown polyoxides grown at 950 and 1050°C.

on single-crystalline silicon by Okada et al.[27] These were attributed to the nitrogen compilation at the oxide/silicon interface for the N_2O oxidation.[28] Here we also found the same result for the N_2O-grown polyoxide for which the SIMS data for nitrogen for the samples are shown in Fig. 2-7. In this figure, the 1050°C N_2O-grown sample had the largest nitrogen concentration in the polyoxide, while the 950°C O_2-grown sample had the minimal amount of nitrogen concentration.

In order to speed up oxide breakdown and reduce testing time, the higher constant current stress 10 mA/cm^2 was selected to apply on the charge-to-breakdown (Q_{bd}) test. Figure 8 shows the dependence of the charge-to-breakdown Q_{bd} (to 50% cumulative failure) under ±10 mA/cm^2 stress on the oxidation temperature for capacitors with N_2O and O_2-grown polyoxides. Although Q_{bd} for the N_2O-grown polyoxide at 950°C is much larger than that for the O_2-grown polyoxide, the Q_{bd} for the N_2O-grown polyoxide decreased with the increasing oxidation temperature, whereas that for the O_2-grown polyoxide increased gradually. This result is similar to the case for the oxide grown on single-crystal silicon in N_2O as reported by Kwong et al.[29,30] This Q_{bd} decrease was attributed to large undulations at the Si/SiO_2 interface to induce the large oxide thinning, which was incurred by the excessive nitrogen incorporation at the Si/SiO_2 interface during N_2O oxidation at higher temperatures, leading to an inhomogeneous oxide growth. This resulted in localized high electric fields leading to smaller Q_{bd}'s.

Figure 9 shows the plots of the electric breakdown field vs the oxide thickness of the range of 85–200 Å for the 950°C N_2O-grown polyoxides. The electric breakdown field decreased with the increase in the polyoxide thickness. This may be due to the longer oxidation time, resulting in a rougher bottom polyoxide/polysilicon interface caused by the enhanced oxidation rate at the grain boundaries[31] despite the incorporated nitrogen at the polysilicon/polyoxide interface. Figure 10 shows the charge trapping characteristics of the 950°C N_2O-grown polyoxides of the thickness of 115, 155, and 197 Å, respectively. For the thinner (115 Å) polyoxide, under the positive constant current stress, there were initially small hole trappings followed by electron trappings. This initial hole trapping diminished as the oxide thickness increased. For the thickest (197 Å) polyoxide, there were no initial hole trappings but electron trappings only. As mentioned previously, hole trappings are due to nitrogen piled-up at the polysilicon/polyoxide interface. For the thinner polyoxide, more nitrogen piled-up at the interface. As polyoxide thickness increased, a longer oxidation time resulted in a rougher interface, leading to larger electron trappings. The Q_{bd} of these samples depended on their electron trappings. The thinner polyoxide, which

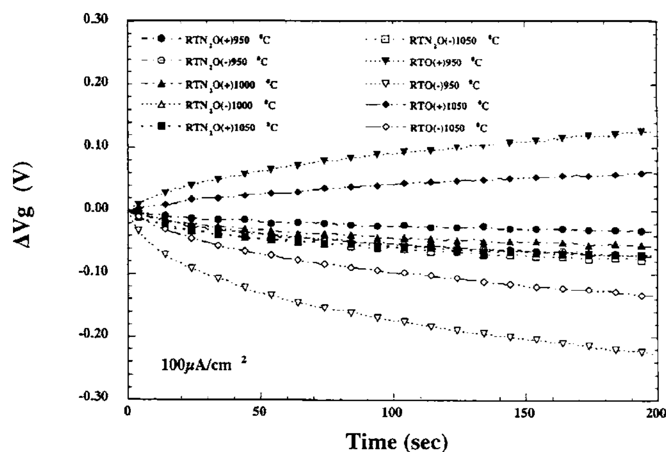

Figure 6. Curves of gate voltage shifts (ΔV_g) vs time of the polyoxides of the N_2O-grown and O_2-grown polyoxides under ±10 mA/cm^2 stressing.

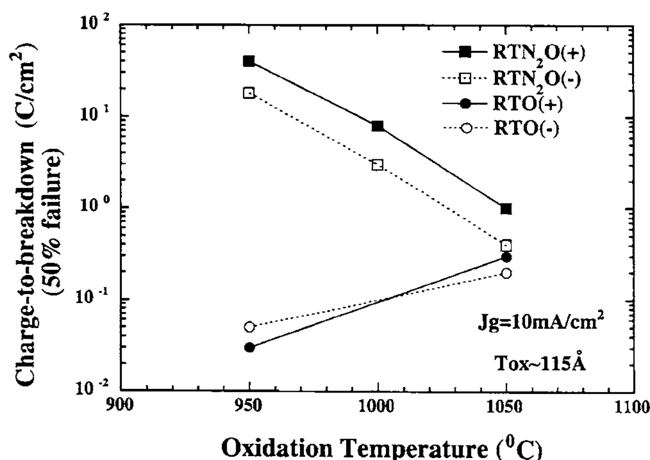

Figure 8. Charge-to-breakdown Q_{bd} (50% cumulative failure) of the N_2O-grown and O_2-grown polyoxides grown at 950–1050°C under ±10 mA/cm^2 stressing.

Downloaded on 2014-04-26 to IP 140.113.38.11 address. Redistribution subject to ECS terms of use (see ecsdl.org/site/terms_use) unless CC License in place (see abstract).

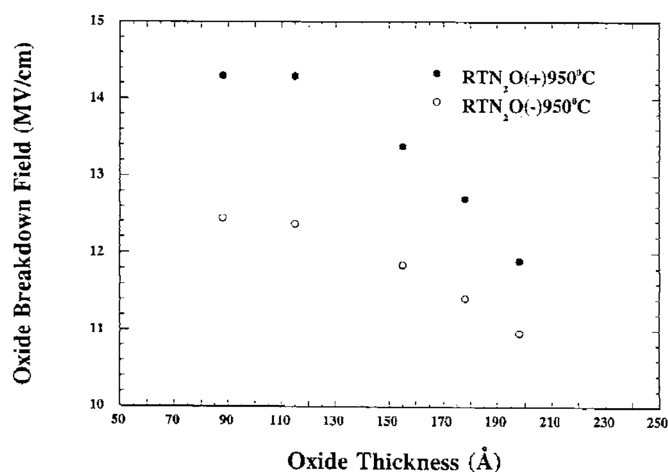

Figure 9. Plots of the electric breakdown field vs polyoxide thickness ranging from 85 to 200 Å for the N_2O-grown polyoxides grown at 950°C.

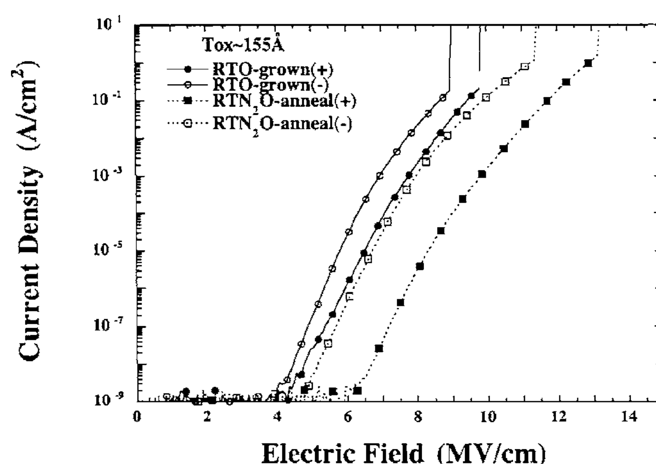

Figure 11. Positive and negative J-E characteristics of the two-step RTP oxidation polyoxides grown at 950°C.

had a lower electron trapping rate, had a larger Q_{bd}; and the thicker polyoxide, which had a higher electron trapping rate, had a smaller Q_{bd}.

In general, the rapid thermal oxidation (RTO)-grown polyoxide has a higher breakdown field (8–9 MV/cm) and reduced leakage current than that grown in the conventional furnace (5–6 MV/cm) due to smoother interface by the rapid thermal process.[32] Furthermore, the RTN_2O-grown polyoxide at moderate growth temperature can reach a high breakdown field (13–14 MV/cm) and low leakage current due to nitrogen incorporated and existing in the interfaces. But when RTN_2O oxidation occurs at higher temperatures, excessive nitrogen incorporated at the Si/SiO_2 interface leads to an inhomogeneous oxide growth and thickness nonuniformity.

In order to improve the thickness nonuniformity of the N_2O-grown polyoxide by RTP, the two-step oxidation, i.e., first RTP oxidizing the polysilicon in O_2 then RTP oxidizing the polyoxide in N_2O, was also investigated.[33,34] With this two-step oxidation process, the amount of nitrogen, which was to be incorporated into the polysilicon/polyoxide interface to improve the polyoxide characteristics, could be well controlled by controlling the duration of the RTP N_2O oxidation at the second step. Figure 11 shows the positive and negative J-E characteristics of the two-step RTP oxidation polyoxides at a temperature of 950°C. It can be seen that the grown polyoxide had significant improvements on both their positive and negative characteristics on the leakage current and the E_{bd} than the O_2-grown polyoxide. In addition, it was also found that the two-step oxidation polyoxide had much improved thickness uniformity, with a thickness deviation of only 5–6 Å (i.e., ~5%), which was similar to that of the O_2-grown polyoxide. Figure 12 shows the charge trappings of the two-step oxidation polyoxide with the O_2-grown polyoxide under the $\pm 100\ \mu A/cm^2$ stress for comparison. The lower current stress $100\ \mu A/cm^2$ was used on the charge trapping for the monitors of the locations and amounts of trapped charges. It is seen that the large electron trapping of the O_2-grown polyoxide can be suppressed by the second-step N_2O oxidation.[35,36]

The centroid of trapped charges, Xt, and the trapped charges, as a function of injected charges, of the two-step oxidation polyoxide and the O_2-grown polyoxide for the positive and negative constant current injections are shown in Fig. 13 and 14, respectively.[37,38] In Fig. 13, one can find that Xt of the two-step oxidation polyoxides was further away from the polyoxide/poly-1 interface than that of the O_2-grown polyoxide. This may be because the nitrogen incorporated at the polyoxide/poly-1 interface released the stress between the polysilicon and the polyoxide, therefore reducing the potential trapping sites near the polyoxide/poly-1 interface. In Fig. 14, one can see that the trapped charges in the two-step oxidation polyoxide were significantly suppressed as compared to the O_2-grown polyoxide. For the polarity dependence of the trapping characteristics, one sees that the electron-trapped charges were higher under the nega-

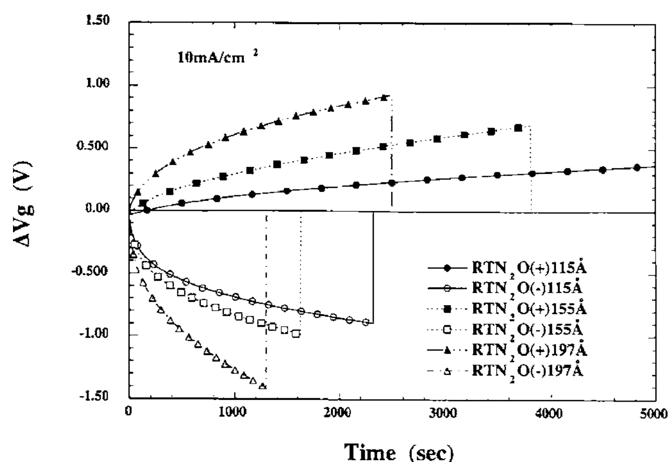

Figure 10. Charge trapping characteristics of the N_2O-grown polyoxides grown at 950°C having thicknesses of 115, 155, and 197 Å, respectively.

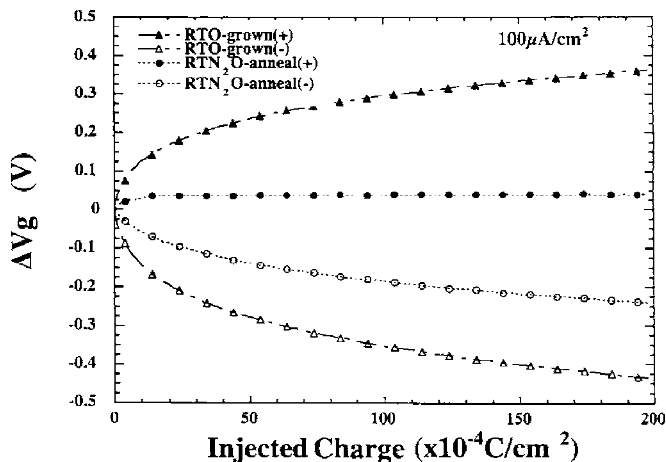

Figure 12. Charge trappings of the O_2-grown and N_2O-anneal polyoxides under $\pm 100\ \mu A/cm^2$ stress.

Downloaded on 2014-04-26 to IP 140.113.38.11 address. Redistribution subject to ECS terms of use (see ecsdl.org/site/terms_use) unless CC License in place (see abstract).

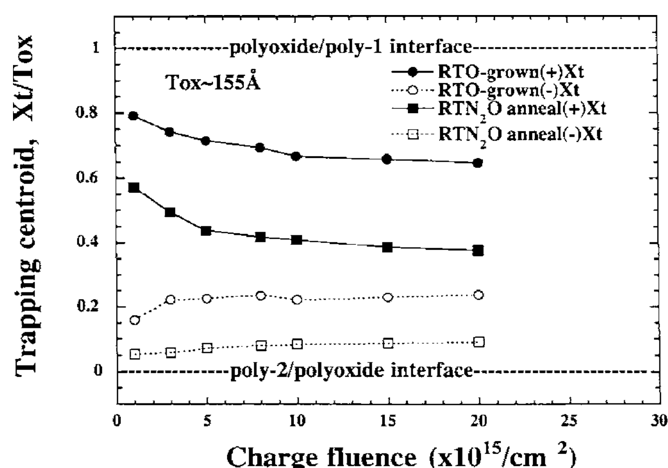

Figure 13. Centroids (Xt) of trapped charges of the O_2-grown and N_2O-anneal polyoxides under ± 100 $\mu A/cm^2$ injections.

tive injection than the positive injection for the two-step oxidation polyoxide, while lower under the negative injection than the positive injection for the O_2-grown polyoxide.

Conclusion

In this paper, we have studied the electrical characteristics of RTP N_2O polyoxides in terms of their oxidation temperature and thickness with O_2 oxidation polyoxides as comparison. AFM, TEM, and SIMS measurements were employed to correlate the electrical characteristics with the physical structures. Results show that RTP N_2O-grown polyoxides exhibit better characteristics than O_2-grown polyoxides on the leakage current, E_{bd}, trappings, and Q_{bd}. It is found that it is the nitrogen incorporated into the polyoxide and at the polyoxide/polysilicon interface during the RTP oxidation process which improves the quality of the polyoxide. The nitrogen in N_2O improves the interface of the polyoxide/polysilicon, thus improving the characteristics of polyoxides. However, the amount of nitrogen incorporated is critical in determining the quality of the polyoxide. Too much nitrogen does not improve but instead degrades the quality of the polyoxide. This was evidenced by the polyoxides, which were RTP oxidized at higher oxidation temperatures had poorer quality due to too much nitrogen in the oxide as revealed by SIMS data. Too high oxidation temperature (1050°C) also causes thickness nonuniformity. Also, initial hole trapping phenomenon during the constant current stress was observed in the N_2O-grown polyoxides. This is also due to the incorporated nitrogen in the polyoxide, because the polyoxides were RTP oxidized at higher temperatures, having more nitrogen inside, and had higher hole trappings. The two-step RTP polyoxides, i.e., the polyoxide is first RTP oxidized in O_2 and then RTP oxidized in N_2O, have better characteristics because a proper amount of nitrogen can be incorporated into the polyoxide at the second oxidation step.

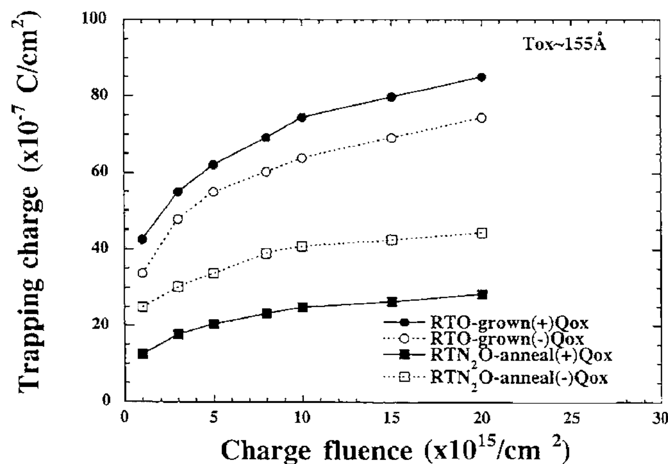

Figure 14. Trapped charges (Qox) of the O_2-grown and N_2O-anneal polyoxides under ± 100 $\mu A/cm^2$ injections.

Chang Gung University assisted in meeting the publication costs of this article.

References

1. T. Ono, T. Mori, T. Ajioka, and T. Takayashiki, *Tech. Dig. - Int. Electron Devices Meet.*, **1985**, 380.
2. S. K. Lai, V. K. Dham, and D. Guterman, *Tech. Dig. - Int. Electron Devices Meet.*, **1986**, 580.
3. R. Stewart, A. Ipri, L. Faraone, and J. Cartwright, Presented at *The IEEE Nonvolatile Semiconductor Memory Workshop*, Vail, CO (1983).
4. N. Mielke, A. Fazio, and H. C. Liou, in *Proceedings of the 1987 IEEE/IRPS*, pp. 85–92 (1987).
5. H. L. Peek and J. F. Verwey, Paper 90 presented at The Electrochemical Society Meeting, San Francisco, CA, May 8–13, 1983.
6. P. A. Heimann, S. P. Murarka, and T. T. Sheng, *J. Appl. Phys.*, **53**, 6240 (1982).
7. L. Faraone, R. Vibronek, and J. Mc Ginn, *IEEE Trans. Electron Devices*, **ED-32**, 577 (1985).
8. L. Faraone, *IEEE Trans. Electron Devices*, **ED-33**, 1785 (1986).
9. S. Mori, N. Arai, Y. Kaneko, and K. Yoshikawa, *IEEE Trans. Electron Devices*, **ED-38**, 270 (1991).
10. C. Cobianu, O. Popa, and D. Dascalu, *IEEE Electron Device Lett.*, **14**, 213 (1993).
11. C. H. Kao, C. S. Lai, and C. L. Lee, *IEEE Electron Device Lett.*, **18**, 526 (1997).
12. C. H. Kao, C. S. Lai, and C. L. Lee, *IEEE Trans. Electron Devices*, **45**, 2238 (1998).
13. S. L. Wu, T. Y. Lin, C. L. Lee, and T. F. Lei, *IEEE Electron Device Lett.*, **14**, 113 (1994).
14. J. H. Klootwijk, H. van Kranenburg, P. H. Woerlee, and H. Wallinga, *IEEE Trans. Electron Devices*, **46**, 1435 (1999).
15. J. H. Klootwijk, M. H. H. Weusthof, H. van Kranenburg, P. H. Woerlee, and H. Wallinga, *IEEE Electron Device Lett.*, **17**, 358 (1996).
16. J. H. Klootwijk, H. van Kranenburg, C. Cobianu, V. Petrescu, P. H. Woerlee, and H. Wallinga, in *Proceedings of the European Solid-State Device Research Conference*, pp. 383–386 (1995).
17. T. F. Lei, J. Y. Cheng, S. Y. Shiau, T. S. Chiao, and C. S. Lai, *IEEE Trans. Electron Devices*, **45**, 912 (1998).
18. P. Candelier, F. Mondon, B. Guillaumont, G. Reimbold, and F. Martin, *IEEE Electron Device Lett.*, **18**, 306 (1997).
19. Z. Liu, H. J. Wann, P. K. Ko, C. Hu, and Y. C. Chang, *Tech. Dig. - Int. Electron Devices Meet.*, **1992**, 625.
20. H. Hwang, W. Ting, D. L. Kwong, and J. Lee, *Tech. Dig. - Int. Electron Devices Meet.*, **1990**, 421.
21. A. Uchiyama, H. Fukuda, T. Hayashi, and T. Iwabuchi, *Tech. Dig. - Int. Electron Devices Meet.*, **1990**, 425.
22. C. S. Lai, T. F. Lei, and C. L. Lee, *IEEE Electron Device Lett.*, **16**, 385 (1995).
23. M. C. Jun, Y. S. Kim, and M. K. Han, *Appl. Phys. Lett.*, **66**, 2206 (1995).
24. T. Y. Chu, W. T. Ting, J. Ahn, and D. L. Kwong, *J. Electrochem. Soc.*, **138**, L13 (1991).
25. C. S. Lai, T. F. Lei, and C. L. Lee, *IEEE Trans. Electron Devices*, **43**, 326 (1996).
26. A. Melik-Martirosian, T. P. Ma, X. W. Wang, X. Guo, F. P. Widdershoven, D. R. Wolters, V. J. D. van der Wal, and M. J. van Duuren, in *VLSI Technology, Systems, and Applications, 2001 International Symposium*, April 18–20, 2001, pp. 138–141.
27. Y. Okada, P. J. Tobin, P. Rushbrook, and W. L. Dehart, *IEEE Trans. Electron Devices*, **41**, 191 (1994).
28. H. Fukuda, T. Arakawa, and S. Ohno, in *Proceedings of the Conference on Solid State Devices Material*, p. 159 (1990).
29. A. B. Joshi, G. W. Yoon, J. Kim, G. Q. Lo, and D. L. Kwong, *IEEE Trans. Electron Devices*, **40**, 1437 (1993).
30. G. W. Yoon, A. B. Joshi, J. Kim, G. Q. Lo, and D. L. Kwong, *IEEE Electron Device Lett.*, **13**, 606 (1992).
31. S. L. Wu, C. Y. Chen, T. Y. Lin, C. L. Lee, T. F. Lei, and M. S. Liang, *IEEE Trans. Electron Devices*, **ED-44**, 153 (1997).
32. G. Q. Lo, A. W. Cheung, and D. L. Kwong, *Appl. Phys. Lett.*, **57**, 1675 (1990).
33. H. Hwang, W. Ting, D. L. Kwong, and J. Lee, *Tech. Dig. - Int. Electron Devices Meet.*, **1990**, 421.
34. A. Bhattacharya, C. Vorst, and A. H. Carim, *J. Electrochem. Soc.*, **132**, 1900 (1985).
35. J. Ahn, W. Ting, T. Chu, S. N. Lin, and D. L. Kwong, *J. Electrochem. Soc.*, **138**, L39 (1991).
36. H. Hwang, W. Ting, B. Maiti, D. L. Kwong, and J. Lee, *Appl. Phys. Lett.*, **57**, 1010 (1990).
37. Z. H. Liu, P. T. Lai, and Y. C. Cheng, *IEEE Trans. Electron Devices*, **38**, 344 (1991).
38. M. S. Liang, N. Radjy, W. Cox, and S. Cagnina, *J. Electrochem. Soc.*, **136**, 3786 (1989).

Downloaded on 2014-04-26 to IP 140.113.38.11 address. Redistribution subject to ECS terms of use (see ecsdl.org/site/terms_use) unless CC License in place (see abstract).